Advances in Science and Technology Research Journal

*Advances in Science and Technology Research Journal*, 2025, 19(1), 390–405
https://doi.org/10.12913/22998624/194889
ISSN 2299-8624, License CC-BY 4.0

Received: 2024.08.14
Accepted: 2024.11.19
Published: 2024.12.01

# Analysis of the possibility of using photovoltaic sources for autonomous cultivation of negatively photoblastic plants

Paweł Mirek[1*], Marcin Panowski[1]

[1] Czestochowa University of Technology, Faculty of Infrastructure and Environment, ul. Generała Jana Henryka Dąbrowskiego 69, Częstochowa, Poland
* Corresponding author's e-mail: pawel.mirek@pcz.pl

## ABSTRACT

Cultivating negatively photoblastic plants requires, first of all, the provision of a constant supply of electricity, without which it is impossible to cyclically implement the process of watering the plants. Due to the large amounts of heat generated by some plants during their growth cyclic watering is not only necessary to provide water for their growth, but also to cool them down. Lack of power supply and failure to water within a certain period leads to overheating of the plants and their destruction, thus necessitating the disposal of the production batch. Ensuring stable power supply and energy security of the cultivation is possible using an island PV plant, but only integrated with appropriately sized energy storage. This paper presents the results of an analysis of the feasibility of using PV sources to ensure continuous cultivation of Mung bean sprouts. Determination of the energy demand of the sprout-growing plant was made based on the developed transient simulation model of the production line. The level of energy demand was determined for different production scenarios. The availability of solar energy at the location of the production line was analyzed and the size of the PV system integrated with energy storage was determined. For full-scale production, regardless of the period of the year in which it is carried out, the maximum energy demand was determined based on simulation studies at 36 kWh/day. For full-scale production, the size of the PV system should be 96.5 kWp, and the capacity of the energy storage should provide weekly coverage of the production line and be about 252 kWh.

**Keywords:** PV systems, autonomous cultivation, transient simulation.

## INTRODUCTION

The European Union's (EU) actions in the area of energy and climate protection stem from key challenges observed concerning ongoing climate change, environmental degradation, and the depletion of conventional fuel resources. Their result is the climate and energy policy, which is built on three pillars, including:

- reduction in the use of energy from primary fuels,
- increasing the use of renewable sources, and
- improving energy efficiency.

EU legislative initiatives setting out principles for achieving climate goals have found expression in several documents, including a set of proposals developed in 2021 called Fit For 55 - FF55 [1]. The package defines climate targets for member states by 2030, including: a reduction in net greenhouse gas (GHG) emissions of at least 55% (compared to 1990 levels), a 40% share of renewable energy sources (RES) in the EU's energy "mix," and a reduction in energy consumption of 39% (relative to primary energy) and 36% (relative to final energy) measured against updated 2020 baseline projections. In 2022, after the Russian invasion of Ukraine, the European Commission developed a strategy to reduce member states' dependence on fossil fuels from the Russian Federation by publishing a document called REPowerEU [2]. It maintains the main assumptions of the FF55 policy while proposing to revise the existing targets for increasing

the share of RES in final energy consumption to 45% and reducing primary and secondary energy consumption by 42.5% and 40%, respectively. The implementation of such targets poses a major challenge to the economic economies of member states, imposing the need not only for the rational use of available energy sources but also for the appropriate management of generated energy resources, especially low-temperature waste heat.

Among all the climate goals defined for the Member States, the greatest intensity of activities can be observed in the area of the use of renewable energy sources, and particular photovoltaics (PV). According to the report [3], the total capacity installed in PV sources in the member states is currently 263 GW, showing a continuously dynamic growth rate of over 40% since 2020 (Fig. 1).

In 2023, the total number of PV installations connected to power grids in Poland exceeded 1.4 million, reaching a total capacity of 11.3 GW [4]. Unfortunately, in recent years, interest in on-grid PV systems has decreased slightly due to changes introduced in the system of accounting for the produced energy. There are also numerous cases of disconnecting PV systems from the grid at times of peak efficiency, which means that the energy system can no longer be treated as a permanently available energy store. In this situation, a discussion was revived about the possibility of returning to the concept of 'energy autarky' proposed by Mueller et al. [5] through the use of energy island systems, also called autonomous or self-sufficiency. Systems of this type are most often built in the form of stand-alone Solar PV installations with energy storage in batteries [6–8] or hybrid systems such as Wind-Pumped hydro, Solar PV-Wind [9–11] or Solar PV-Wind-Biomass [12], also with energy storage in batteries. Autonomous power systems are of particular interest, especially in areas where access to the power grid is problematic. Examples of such places are inhabited, non-urbanized areas [13] and difficult-to-reach or isolated areas [14, 15]. Systems of this type are also considered in regions where, due to appropriate weather conditions, the ambitious goal of achieving energy independence from fossil fuels and supplying energy from the grid is pursued [16].

In recent years, a dynamic increase in the use of photovoltaic solar systems in agricultural crops has been observed. Its aim is primarily to reduce the energy consumption of installations ensuring the creation of the required microclimate for plant growth and to increase the safety of the production process. In the process of growing plants, photovoltaic installations can be used independently or as hybrid installations (Fig. 2):

- with PV-GHP geothermal sources (Photovoltaic-Geothermal Heat Pump),
- cooperating with deep-well pumps in PV-WP (Photovoltaic Water Pumping) irrigation systems,
- supporting the operation of PV-H (Photovoltaic-Heating) heating systems,

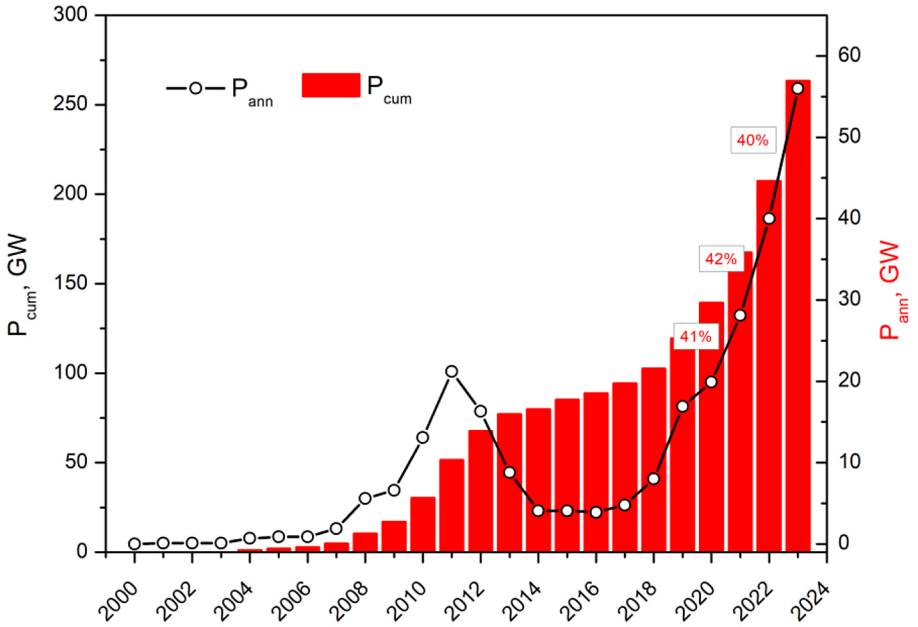


**Figure 1.** Annual ($P_{ann}$) and cumulative ($P_{cum}$) values of installed capacity in photovoltaic panels in EU member states. Adapted based on [3]

- supporting the operation of PV-C (Photovoltaic-Cooling) cooling systems
- powering artificial lighting systems that intensify plant growth PV-L (Photovoltaic-Lighting),
- powering cooling devices used to cool PV-RS greenhouses (Photovoltaic Refrigeration System).

An example of the application of a PV-GHP system serving as a heat source for a greenhouse can be found in the installation described by Russo et. al [17]. The operation of the system was compared in terms of environmental impact with a heat preparation system based on liquefied petroleum gas. The study analyzed the amount of heat produced, microclimatic conditions, and the level of electricity used, showing that the PV-GHP system emitted 50% less carbon dioxide and showed an energy payback time of only 1 year. In the work of Sonnevald et al. [18] demonstrated the possibility of using PV systems as heat preparation systems (PV-H) for cultivation in a greenhouse. The study used a new type of greenhouse, which utilizes the phenomenon of reflecting solar radiation in the near-infrared (NIR) range with simultaneous electricity generation using a hybrid system consisting of PV cells and thermal collectors. According to the analysis, the system demonstrated a capacity for annual electricity production of 20 kWh/m$^2$ and heat production of 160 kWh/m$^2$. These values proved sufficient for the installation to operate fully autonomously independent of fossil fuel combustion heat preparation equipment. PV systems can also serve as stand-alone installations for dissipating excess heat gains from controlled cultivation space (PV-C). An example of this type of installation was described by Al-Shamiry et al. using 48 PV panels with a unit power of 18.5 W working together with a bank of 12 batteries, providing the power source for two 400 W fogging fans [19]. As demonstrated, the system could provide power in a set time regime without using energy from the power grid. Various types of devices are used in PV-C hybrid systems. In addition to traditional fans, they can also be:

- underground air tunnels used in ground-air heat exchangers [20],
- systems of horizontal pipes laid in the ground [21],
- complete air conditioning systems.

Lighting plays an important role in controlled plant cultivation installations. PV-L installations can act as systems supporting power supply in crops of positively photoblastic plants and in greenhouse systems during periods of significant light deficit, i.e. in winter. In greenhouse crops, systems of this type usually have an additional purpose, providing energy for autonomous cooling systems in the summer [22]. Recently, there has been an increased interest in autonomous PV-WP systems used to irrigate crops located in remote and desert regions. Among all technologies for the use of photovoltaics in the field of agricultural crops, this type of system has so far gained

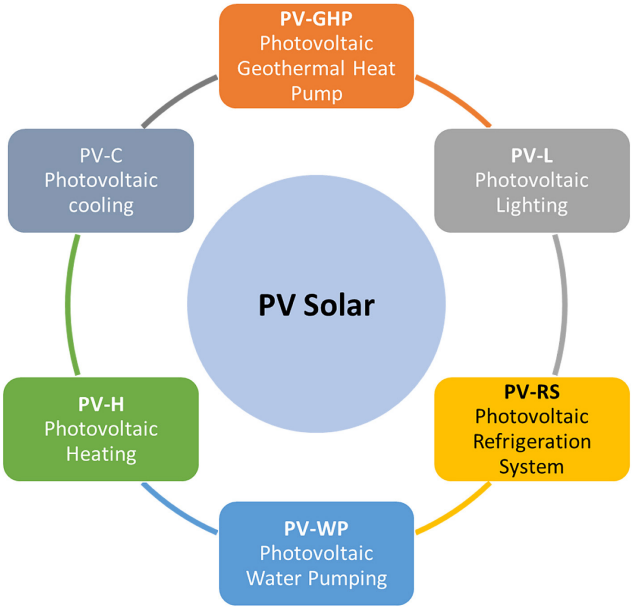


**Figure 2.** Technologies of photovoltaic solar systems used in plant cultivation

the greatest application possibilities. Examples of such installations are well documented in the literature [23–25], and their basic purpose is to provide the required water flow at specific times of the day depending on weather conditions, the size of the PV installation, and the capacity of the water tank. An important role in PV-WP systems is played by control algorithms which, based on many years of experience, have achieved the ability to control the operation of the installation in a way that fully protects the crop against excessive water deficit in various weather conditions [26–27].

In summary, it should be stated that the use of autonomous power systems in the field of crops based on PV solar technology is very popular especially where:

- access to the electricity grid is difficult,
- meteorological conditions favor the construction of island systems,
- the production process of crop cultivation is carried out with a high level of power supply reliability.

Autonomous systems are most often built as hybrid power systems, where, in addition to energy from the Sun, heat stored in the ground is also used.

The aim of the paper is to analyze the possibility of using an autonomous power supply system based on PV solar technology in a temperate climate zone providing the energy necessary for growing negatively photoblastic Mung bean sprouts in conditions of a high level of energy supply reliability.

## TECHNOLOGY OF MUNG BEAN CULTIVATION

The Mung bean (Vigna radiata) belongs to the group of legumes, which are a valuable source of protein and exogenous amino acids. The sprouts of this plant are characterized by particularly high nutritional values and their production period under controlled cultivation lasts from 5 to 7 days. Since Mung bean seeds are classified as negatively photoblastic, they germinate in complete darkness and specific microclimatic conditions. Therefore, the growth chamber must be periodically ventilated with warm air to remove excess carbon dioxide, and the germinating grains must be watered at a set time interval with water at a temperature exceeding 20 °C. Since the preparation of significant amounts of warm air and water for the cultivation of sprouts involves a large energy expenditure, this process is carried out in a technological system that uses energy recovery from the process of watering

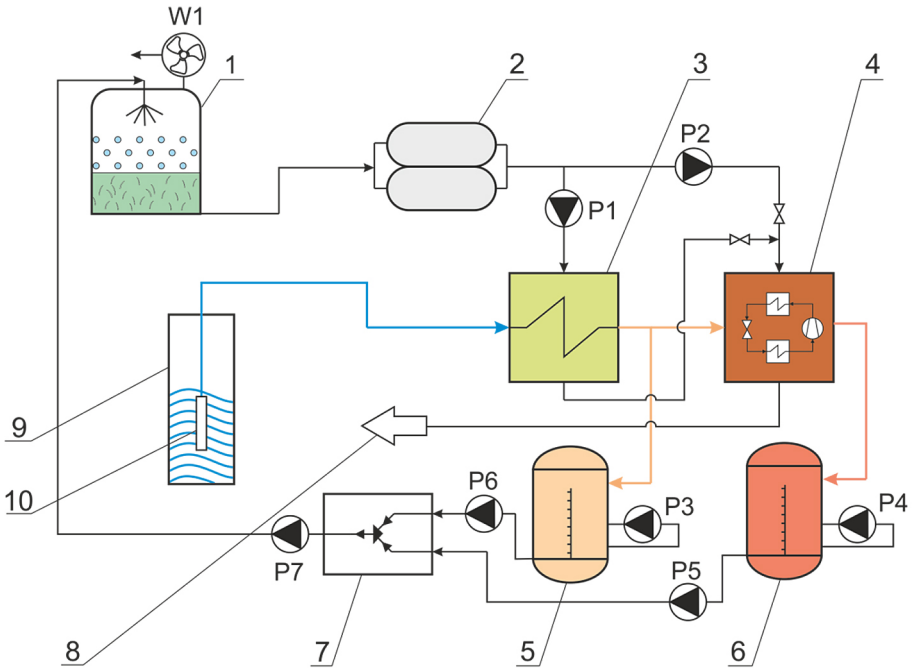


**Figure 3.** The simplified scheme of water and air pretreatment for cultivation of Mung bean sprouts. 1-growing room, 2-waste heat accumulator, 3-1st stage heat exchanger, 4-heat pump with 2nd stage heat exchanger, 5-cold water tank, 6-hot water tank, 7-mixer, 8-dirty water outlet, 9-deep well, 10-submesible pump, W1-exhaust fan, P1-P7-circulation pump

plants, which uses a complex set of heat exchangers cooperating with a heat pump [28].

## Cultivation process organization

Figure 3 shows a simplified technological diagram of the air and water preparation installation for the production of Mung bean sprouts.

Freshwater at temperature of 9 °C drawn from deep well 9, is pumped into heat exchanger 3. The heating medium in heat exchanger 3 is wastewater at a temperature of 23 °C fed from heat accumulator 2. The second stage of heating freshwater is heat pump 4, to which wastewater from heat accumulator 2 is also fed. In heat pump 4, heat from wastewater is transferred to freshwater, which as a result is heated to 31 °C. The freshwater heated in heat exchanger 3 is stored in cold water storage tank 5, while the water heated in heat pump 4 is stored in hot water storage tank 6. Water for watering vegetable sprouts is prepared in mixer 7, in which two streams of water coming from tanks 5 and 6 are mixed. The proportions of mixing water in the mixer result from different scenarios implemented by a dedicated controller, so that the temperature of water for watering is contained in the range of 19–31 °C. The prepared freshwater is then pumped into growth chamber 1, where the growing sprouts are watered. The growth chamber must be periodically ventilated using the W1 exhaust fan to bring in oxygen and remove excess carbon dioxide. As can be seen from Figure 3, the stand-alone operation of the plant involves a power source for circulating pumps, valve actuators (not visible in Fig. 3), and automatic control systems. These devices operate in full automation mode implementing various production scenarios as a function of both production volumes and external weather conditions.

## Energy demand of production line

Preparation of water and air for the process of growing Mung bean sprouts according to the presented scheme (Fig. 3) was implemented in an industrial installation with a nominal capacity of approximately 108 tons of Mung bean sprouts per week. For the purpose of analyzing and optimizing the process, as well as determining the energy demand of the installation in various production variants, a simulation model of the installation for transient states was developed. FLOWNEX® Simulation Environment (FlownexSE) software was used to formulate the simulation model, which is an advanced simulation environment that allows for complex analyses, simulations, design, and optimization of various types of systems, in particular thermal-flow systems. FlownexSE software enables:

- creating models using, among others, two-phase and non-Newtonian fluids, suspensions, gases, gas mixtures and insoluble mixtures
- adding user-defined components, MS Excel sheets, optimizing or combining calculations with other engineering software
- modeling of heat transfer processes, mechanical subsystems, control systems and electrical networks
- automatic calculation of parameters of system elements to obtain specific operating conditions of the installation.

Simulations in the Flownex software are based on solving partial differential equations for the conservation of mass, momentum and energy (Equations 1÷3, respectively). Solving these equations allows for determining the distributions of mass flow, pressure and temperature in the entire simulated system in the 1D domain:

$$\frac{\partial \rho}{\partial t} + \frac{\partial}{\partial x}(\rho V) = 0 \tag{1}$$

$$\frac{\partial(\rho V)}{\partial t} + \frac{\partial(\rho V^2)}{\partial x} = -\frac{\partial p}{\partial x} - \rho g \frac{\partial z}{\partial x} - \frac{f \rho |V| V}{2D} \tag{2}$$

$$\frac{\partial(\rho(h_o + gz) - p)}{\partial t} + \frac{\partial(\rho V(h_o + gz))}{\partial x} = \dot{Q}_H - \dot{W} \tag{3}$$

where: $\rho$ – fluid density [kg/m$^3$]; $t$ – time [s]; $x$ – element length [m]; $V$ – fluid mean velocity [m/s]; $f$ – friction factor [-]; $z$ – height [m]; $g$ – acceleration due to gravity [m/s$^2$]; $p$ – pressure [Pa]; $D$ – pipe internal diameter [m]; $h_0$ – stagnation enthalpy [J]; $\dot{Q}_H$ – heat flux [W]; $\dot{W}$ – mechanical work [W].

The general balance equations presented above constitute the basic equations of each element of the model. Depending on the specific component, they are supplemented with additional model equations specific to a given device. One of the main elements of the simulation model in the part covering the heat recovery system is the plate heat exchanger (HE1), which is responsible for the recovery of low-temperature waste heat. The exchanger model consists of two components, heat exchanger primary (HEP) and heat

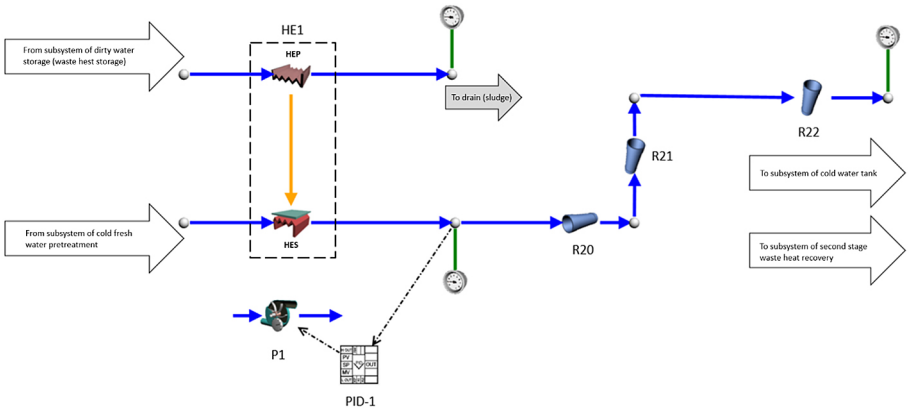


**Figure 4.** Part of simulation model – flat plate heat exchanger subsystem

exchanger secondary (HES). The first one represents the primary side and the second one the secondary side of the device (Fig. 4).

Additional model equations describing the heat exchange process in such an exchanger are represented by relationships (4) – (7) and result not only from the specificity of the modeled heat exchanger but also from the method used to solve its model equations. Thus, for example, an additional equation in the momentum balance determining the pressure drop of streams flowing through the heat exchanger is the relationship:

$$\Delta p_0 = C_k \rho^{\beta} Q^{\alpha} \tag{4}$$

where: $C_k$, $\alpha$, $\beta$ – pressure loss constants [-]; $\rho$ – fluid density [kg/m$^3$]; $Q$ – volumetric fluid flow rate [m$^3$/s].

FlownexSE uses the NTU (Number of Transfer Units) method to calculate the heat flow through the heat exchanger. This method allows the calculation of energy exchange in the device without knowing the fluid temperatures at its outlet and does not require providing details of the heat exchanger geometry. The heat flux is determined from the equation:

$$\dot{Q}_H = \varepsilon \left(\dot{m} c_p\right)_{min} (T_{i,min} - T_{i,max}) \tag{5}$$

where: $\varepsilon$ – heat exchanger performance [-]; $\dot{m}$ – mass flow rate [kg/s]; $C_p$ – specific heat [J/kgK]; $T_{i,min}$ – temperature of heated fluid at the heat exchanger inlet [K]; $T_{i,max}$ – temperature of heating fluid at the heat exchanger inlet [K].

For any heat exchanger, the performance ε can be expressed as a function of two variables:

$$\varepsilon = f\left(NTU, \frac{C_{min}}{C_{max}}\right) \tag{6}$$

where: $NTU$ – number of heat transfer units, [-];
$C = \dot{m} \cdot c_p$ – heat capacity flux, [W/K].

NTU represents the number of heat transfer units and is defined as follows:

$$NTU = \frac{AU}{C_{min}} \tag{7}$$

where: $AU$ – product of heat transfer area and heat transfer coefficient, [W/K].

The developed model took into account all installation elements involved in the normal production of sprouts, in particular pumps, tanks, heat exchangers, valves and pipelines. To reliably reflect the real installation, the geometric and operational characteristics of the used devices were implemented in the model taking into account the full geometry of all pipelines. Example fragments of the model including subsystems of cold and hot water tanks are presented in Fig. 5 and Fig. 6 respectively.

Figure 5 shows the subsystem of the hot water tank, which stores water heated in a two-stage system. The water is heated first in the heat exchanger HE1, and then in the exchanger HE2 (see Fig. 3). The control valve EV2 is responsible for filling the HWT tank. This valve is opened when the level of hot water in the HWT tank drops below the lower limit and closed when the water level reaches the upper limit. The opening and closing of the EV1 valve is controlled by the HWLC controller. The water recirculation system to the HWT tank operates when the EV2 valve is open (the control system P4 is not shown in the figure) to maintain a constant temperature in the HWT tank. The hot water pump P5 supplies hot water to the MX mixer, where hot and cold water are mixed to obtain the required temperature of the water used for irrigation. The cold water tank

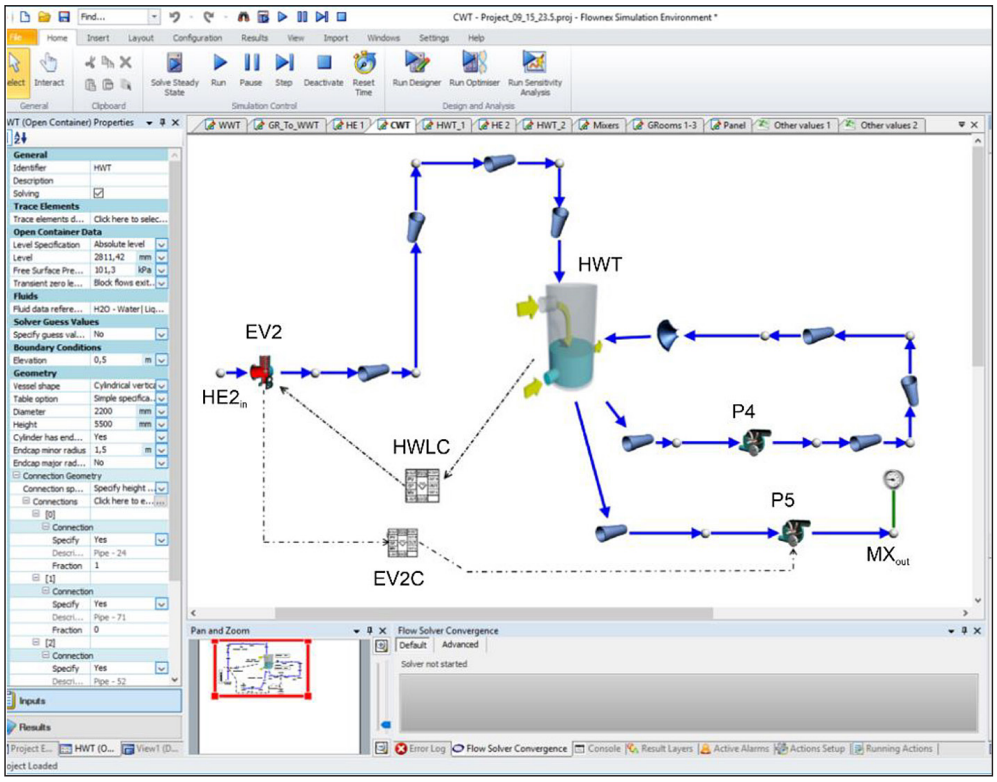


**Figure 5.** Part of the simulation model – hot water tank subsystem. $HE2_{in}$ – inlet from heat exchanger HE2, EV2 – hot water electronic valve, HWT – hot water tank, HWLC – hot water tank water level control, EVC2 – hot water electronic valve (EV2) control, P4 – hot water tank recirculation pump, P5 – hot water pump, $MX_{out}$ – hot water outlet to water mixer MX

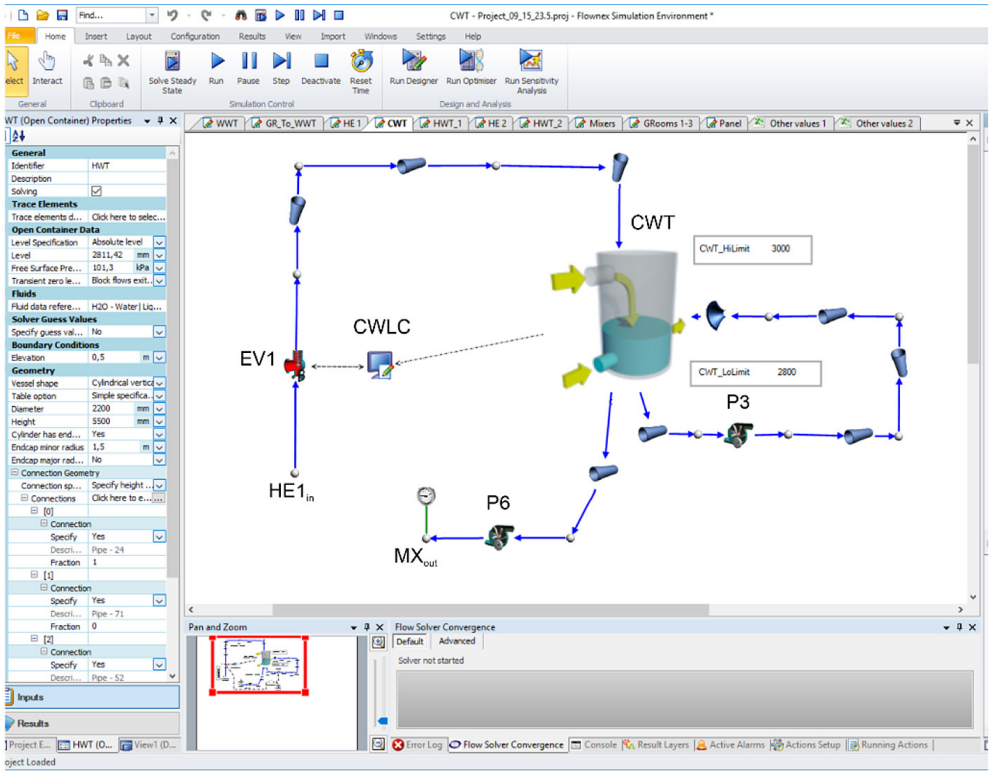


**Figure 6.** Part of the simulation model – cold water tank subsystem. $HE1_{in}$ – inlet from heat exchanger HE1, EV1 – cold water electronic valve, CWT – cold water tank, CWLC – cold water tank water level control, P3 – cold water tank recirculation pump, P6 – cold water pump, $MX_{out}$ – hot water outlet to water mixer MX

subsystem shown in Figure 6 is operated similarly however the water stored in this tank is heated only in the HE1 exchanger (compare Fig. 3).

The developed simulation model was validated based on real data collected on the installation operating under normal production conditions and then used to determine the energy demand of the system for various production scenarios. A more in-depth description of the real installation, as well as the simulation model, can be found in [28–31]. For validation purposes, the measurement data were derived from the real object DCS system, and additional measurements were performed to obtain nonregistered in DCS database values. A detailed description of the measurements performed and the model validation process can be found in [29, 31]. In particular, the calculations were carried out for different watering times and periods, as well as with variable production levels. The analyzed variants are summarized in Table 1 and Table 2.

In variants presented in Table 1, both the watering time and duration apply to one growth chamber. For each production level of the cultivation line, calculations were carried out for each of the three production variants, which resulted in obtaining the energy demand of the line in 9 operational variants. Each time, the calculations were carried out for one full day of cultivation.

**Table 1.** Analyzed watering schemes

| Case | Watering time [min] | Watering period [min] |
|---|---|---|
| PC1 | 10 | 230 |
| PC2 | 15 | 225 |
| PC3 | 20 | 220 |

**Table 2.** Analyzed production line yield

| Case | Production level [%] | Production level [tons/week] |
|---|---|---|
| PL1 | 17 | 18 |
| PL2 | 50 | 54 |
| PL3 | 100 | 108 |

Obtained distributions of instantaneous electricity demand for all variants PL3 (watering time 20, 15, and 10 min, line efficiency 100%), PL2 (watering time 20, 15 and 10 min, line efficiency 50%) and PL1 (watering time 20, 15, and 10 min, line efficiency 17%) are presented in Figures 7– 9, respectively.

It should be emphasized that the technological line for growing sprouts has been configured in such a way that between subsequent waterings the freshwater in the cold and hot water tanks is fully replenished, which makes the cycle of the installation's electricity demand repeatable, assuming that the production scheme remains

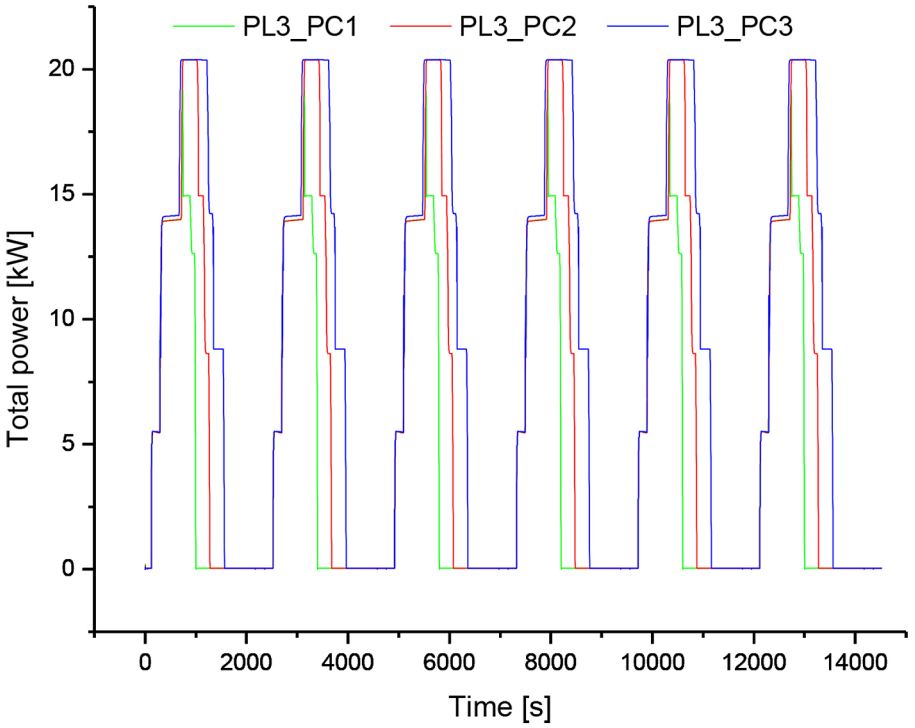


**Figure 7.** Distribution of instantaneous demand for electricity for all PL3 production schemes

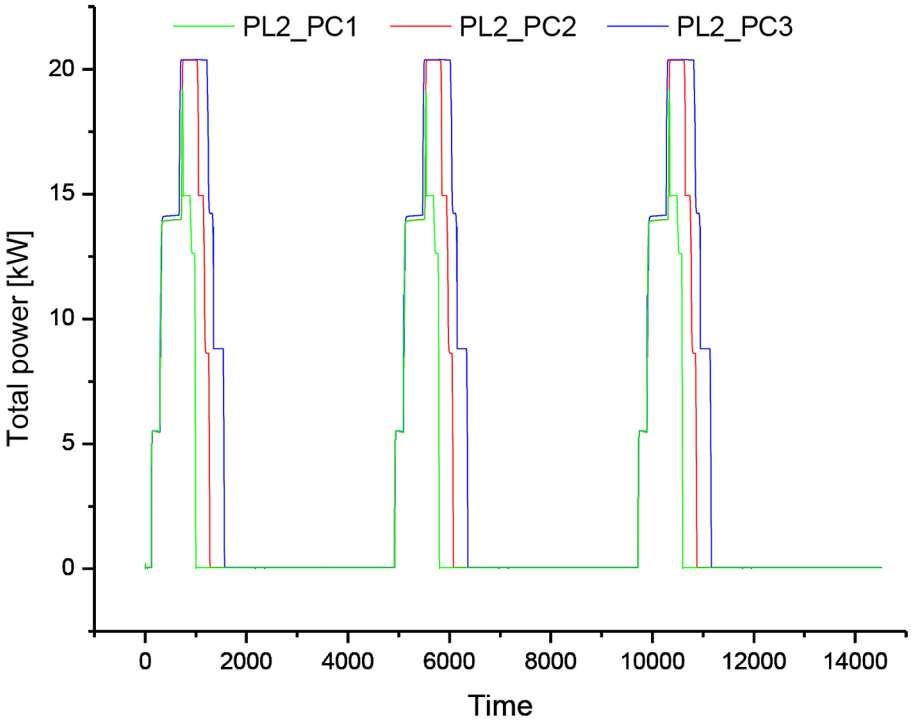


**Figure 8.** Distribution of instantaneous demand for electricity for all PL2 production schemes

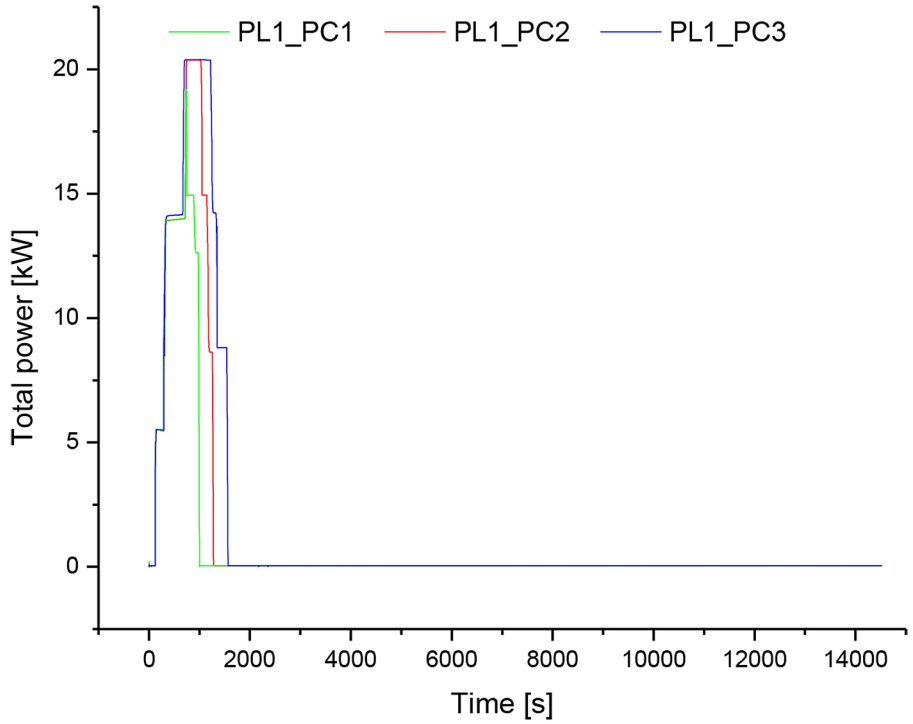


**Figure 9.** Distribution of instantaneous demand for electricity for all PL1 production schemes

unchanged. The cumulative daily energy demand of the sprout cultivation installation for all analyzed production scenarios is shown in Figure 10. The daily demand includes the electricity consumption (related to the cultivation process) of the heat pump, which generates heat mostly for the processes not connected with cultivation. Since the heat pump operates at constant conditions, its value is approximately constant and equal to 7.5. Based on the calculations results obtained it was assessed that the average heat pump daily electricity consumption related to the cultivation of

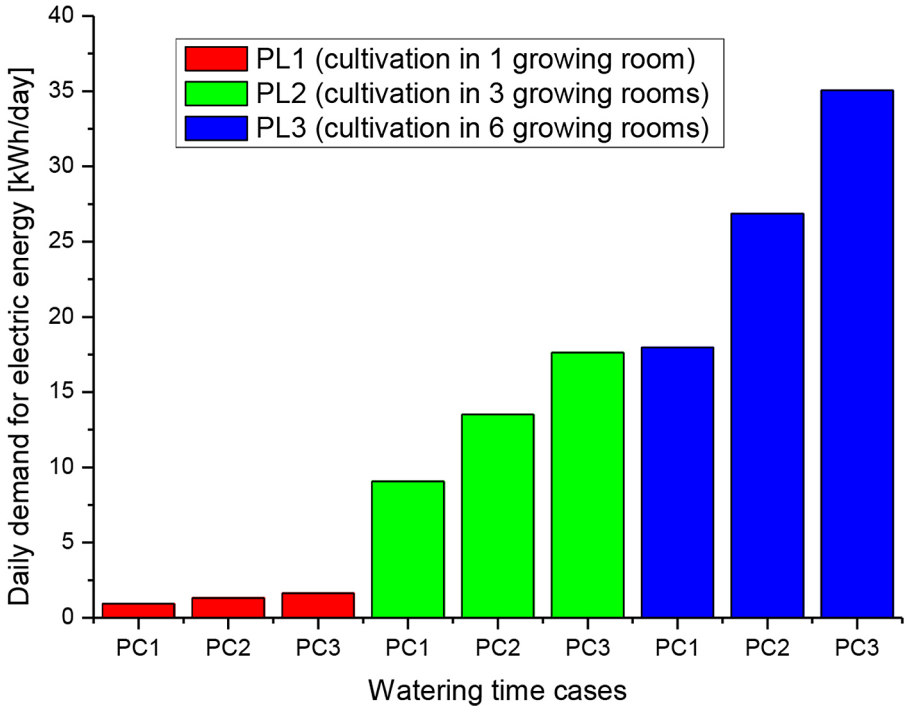


**Figure 10.** Cumulative daily demand for electricity for different production schemes

sprouts is about 3.16 kWh for cultivation in full production scale (in 6 growing rooms), 1.28 kWh for cultivation in 3 growing rooms and 0.26 kWh for cultivation in 1 growing room. The highest demand for electrical energy of the installation is, of course, observed for the case of the full capacity of the production line and the longest watering time, i.e. in the production variant marked PL3_PC3. In this case, the daily electricity demand is about 36 kWh. Since this demand does not depend on weather conditions (i.e. the time of year in which production is carried out) but only on the adopted production scenario and the scale of production, the off-grid PV system powering such an installation should provide a sufficient amount of energy also in winter periods, when the available the amount of solar energy is the least.

## SOLAR ENERGY RESOURCES AT THE INSTALLATION LOCATION

To determine the possibility of energy security of an installation for growing negatively photoblastic plants using an off-grid PV system, it is necessary not only to determine the characteristics of the installation's energy demand but also the availability of solar energy resources in the place where it is located. The assessment of these resources is based on weather data of a typical meteorological year (TMY) [32], which include, among others, data on the intensity of solar radiation reaching the earth on an hourly basis, taking into account the orientation of the photovoltaic system concerning the cardinal directions and the angle of inclination of photovoltaic panels to the horizontal. Since TMY data are not available for every location, the calculations used data from the nearest weather station (straight line distance ca. 15 km). Figure 11 presents the cumulative daily sums of available solar radiation energy values, related to 1 $m^2$ of area, determined for the data of a typical meteorological year and measured in the area of the sprout cultivation installation.

Data from the real PV system depicted in Figure. 11 were obtained from the three consecutive years of the system operation (i.e. 2019–2021) and represent their average values. Production values for TMY data were estimated assuming an average efficiency of PV panels to be 17%. As indicated, electricity production from the real installation differed significantly in the analyzed periods from the average production determined based on TMY data. It is visible that the years 2019–2021 showed a significantly higher level of available energy compared to previous years. It can therefore be expected that the size of the PV installation determined based on TMY data will be characterized by a higher energy yield, and

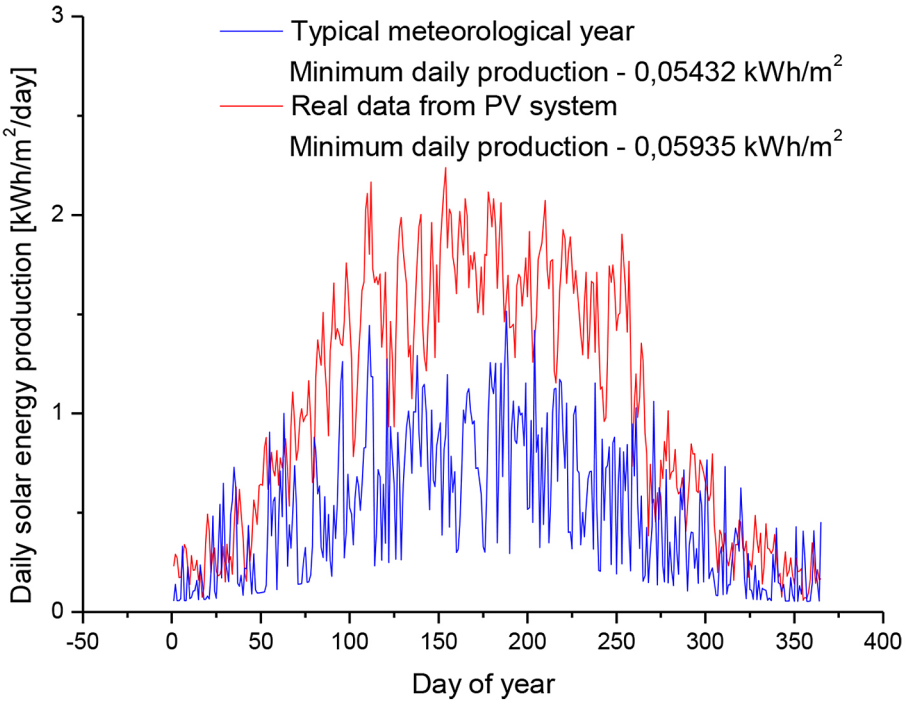


**Figure 11.** Daily solar energy production from TMY and real PV system

therefore determining the number of installations based on TMY data will have a certain safety margin concerning demand.

## OFF-GRID PV SYSTEM SIZE

Energy security of the production line for growing vegetable sprouts by using an island PV system requires correlating the energy demand of the production line with the availability of solar energy. As indicated earlier, the extreme case of the energy demand of the production line is the cultivation of the sprouts carried out at full capacity, i.e. nominal efficiency, corresponding to the PL3 production scheme. At the same time, the longest watering time for sprouts (PC3 scheme) results in the highest consumption of freshwater and the longest operating time of pumps replenishing water reserves in cold and hot water tanks. For this production scheme (i.e. PL3_PC3), the daily electricity demand is 36 kWh. Due to the continuity of the production, regardless of the availability of energy from the PV system and assuming an off-grid work of installation without electricity storage, the size of the PV system should be determined based on the minimum value of available solar energy, which is approximately 0.05432 kWh/m$^2$. Table 3 lists the working surface of three types of PV panels with different nominal powers along with their quantity required to cover the demand of the production line. As can be seen, to fully cover the demand of the sprout cultivation installation, the total working area of PV panels should not be less than ca. 663 m$^2$.

However, since the cultivation of negatively photoblastic plants requires a continuous power supply, it is necessary to equip an off-grid PV system with an additional electricity storage module. The capacity of such an electricity storage system should be considered not only from the point of view of the energy security of the crop but also from the point of view of minimizing the size of the PV installation. For this purpose, the

**Table 3.** Required size of PV system

| PV peek power | PV peek power | Single PV panel working surface | PV panels count |
|---|---|---|---|
| [$W_p$] | [$W_p$/m$^2$] | [m$^2$] | [-] |
| 300 | 224 | 1.34 | 495 |
| 400 | 225 | 1.78 | 373 |
| 500 | 226 | 2.21 | 300 |

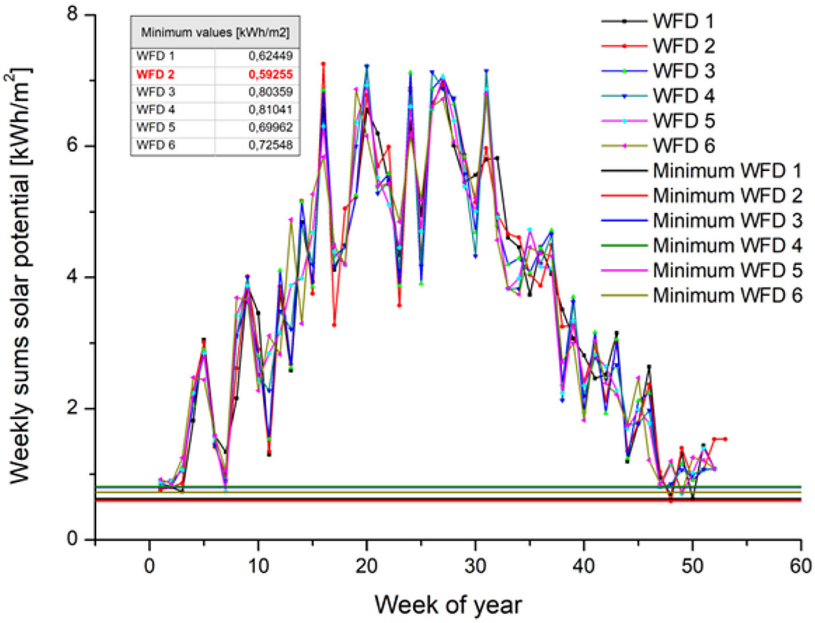


**Figure 12.** Weekly sums of solar energy

availability of solar energy in weekly cycles was analyzed, which allowed to determine the potential for storing energy from the PV system. Figure 12 shows the distribution of available solar energy in weekly cycles.

The smallest available amount of solar energy from one square meter of the PV system is 0.59255 kWh, while the weekly demand of the production line is approximately 252 kWh. Therefore, to fully cover the demand of the sprout cultivation installation, the total working area of photovoltaic panels integrated with the energy storage should not be less than approximately 426 $m^2$. Table 4 and Table 5 summarize the required number of panels of various powers and the total power of the PV system for different variants based on daily and weekly data. Table 5 lists the sizes of the PV systems determined based on the

**Table 4.** Required size of PV system according to weekly demand

| PV peek power | PV peek power | PV panel working area | PV panels count |
|---|---|---|---|
| [$W_p$] | [$W_p/m^2$] | [$m^2$] | [-] |
| 300 | 224 | 1.34 | 318 |
| 400 | 225 | 1.78 | 240 |
| 500 | 226 | 2.21 | 193 |

**Table 5.** PV system total peek power

| PV peek power | PV peek power | PV panels count | PV system total peek power |
|---|---|---|---|
| [$W_p$] | [$W_p/m^2$] | [-] | [$kW_p$] |
| Based on daily demand (PV system without energy storage) | | | |
| 300 | 224 | 495 | 148 500 |
| 400 | 225 | 373 | 149 200 |
| 500 | 226 | 300 | 150 000 |
| Based on weekly demand (PV system with energy storage) | | | |
| 300 | 224 | 318 | 95 400 |
| 400 | 225 | 240 | 96 000 |
| 500 | 226 | 193 | 96 500 |

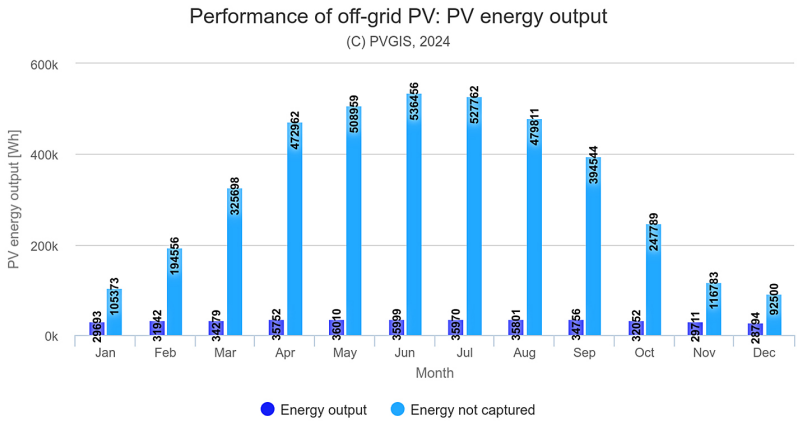


**Figure 13.** Monthly analysis of production and consumption for 36 kWh energy storage

daily demand of the production line (PV system without energy storage) and the weekly demand of the production line (PV system with energy storage). As can be seen, the energy storage allows for a significant reduction of the size of a photovoltaic installation (ca. 36%). Figure 13 and Table 6 present an exemplary analysis of monthly balances of energy production and consumption for the PV system with the capacity of 150 $kW_p$ and 36 kWh energy storage, respectively [33].

As can be seen, in the case of the PV system equipped with an energy storage with a capacity corresponding to the daily demand the battery remains empty almost 62% of the time, and the average energy shortage to maintain production is at the level of 4.2 kWh. Table 7 and Table 8 present a summary of production and consumption of the energy for the PV system with

**Table 7.** PV system 150 kWp and battery 252 kWh

| Provided inputs | Parameter |
|---|---|
| Location [Lat/Lon] | 50.901,19.417 |
| Horizon | Calculated |
| Database used | PVGIS-SARAH2 |
| PV installed [Wp] | 150000 |
| Battery capacity [Wh] | 252000 |
| Discharge cut-off limit [%] | 40 |
| Consumption per day [Wh] | 36000 |
| Slope angle [°] | 30 |
| Azimuth angle [°] | 0 |
| Simulation outputs | Parameter |
| Percentage of days with fully charged battery [%] | 97.29 |
| Percentage of days with empty battery [%] | 0 |
| Average energy not captured [Wh] | 341038.55 |
| Average energy missing [Wh] | 0 |

**Table 6.** PV system 150 kWp and battery 36 kWh

| Provided inputs | Parameter |
|---|---|
| Location [Lat/Lon] | 50.901,19.417 |
| Horizon | Calculated |
| Database used | PVGIS-SARAH2 |
| PV installed [Wp] | 150000 |
| Battery capacity [Wh] | 36000 |
| Discharge cut-off limit [%] | 40 |
| Consumption per day [Wh] | 36000 |
| Slope angle [°] | 30 |
| Azimuth angle [°] | 0 |
| Simulation outputs | |
| Percentage of days with fully charged battery [%] | 98.87 |
| Percentage of days with empty battery [%] | 61.89 |
| Average energy not captured [Wh] | 338222.59 |
| Average energy missing [Wh] | 4188.11 |

**Table 8.** PV system 96.5 kWp and battery 252 kWh

| Provided inputs | Parameter |
|---|---|
| Location [Lat/Lon] | 50.901,19.417 |
| Horizon | Calculated |
| Database used | PVGIS-SARAH2 |
| PV installed [Wp] | 96500 |
| Battery capacity [Wh] | 252000 |
| Discharge cut-off limit [%] | 40 |
| Consumption per day [Wh] | 36000 |
| Slope angle [°] | 30 |
| Azimuth angle [°] | 0 |
| Simulation outputs | Parameter |
| Percentage of days with fully charged battery [%] | 90.25 |
| Percentage of days with empty battery [%] | 0.34 |
| Average energy not captured [Wh] | 222346.46 |
| Average energy missing [Wh] | 13212.45 |

a capacity of 150 $kW_p$ and 96.5 $kW_p$, respectively, equipped with an energy storage facility with a capacity equal to the weekly demand of the production line.

As can be seen from the data presented in the tables, in the case of smaller PV systems equipped with a larger battery, the number of days in which the energy storage is empty decreases significantly, but the average value of energy shortage increases almost three times. However, in the case of a larger PV system and a larger energy storage facility, there are no days when concerning demand the energy storage facility is empty and when shortages of energy from the PV system occur.

## CONCLUSIONS

Ensuring stable power supply and energy security of the cultivation of Mung bean sprouts is crucial for avoiding potential loss of batch of production. The paper presents the analysis of the possibility of using an island PV installation equipped with energy storage to cover the demand from the cultivation line for electricity. Therefore, the detailed simulation model of the cultivation line was elaborated, validated based on data acquired from real installation, and used in the simulation experiment to assess the electricity demand of the cultivation line, at different production scenarios. The results obtained show, that to fully secure production, regardless of the period of the year in which it is carried out, the maximum energy demand (full-scale production) is at the level of 36 kWh/day.

The comparison analysis of solar energy potential based on TMY data and real PV system shows that electricity production from the real PV systems may be expected as significantly higher than the average production determined based on TMY data. Therefore, the size of the PV installation determined based on TMY data will be oversized, which will lead to a certain safety margin concerning demand. The analysis of the stand-alone PV system equipped with energy storage, according to the PV system pick power vs. energy storage capacity relation, shows that the larger the capacity of the energy storage system, the lower the pick power of the PV system. Moreover, covering total electricity demand (for full production scale) from the stand-alone PV system is possible. In that case, the pick power of the photovoltaic system should be at least 96.5 kWp, while the capacity of the energy storage should ensure weekly coverage of the production line's demand and amount to approximately 252 kWh.

### Acknowledgment

The research presented in this paper was financially supported by National Centre for Research and Development under the projects POIR.01.01.01-00-0759/17 and POIR.01.01.01-00-0058/19, as well as by the statute subvention of Czestochowa University of Technology, Faculty of Infrastructure and Environment.

## REFERENCES

1. Communication from the European Commission of 14/07/2021 to the European Parliament, the Council, the European Economic and Social Committee and the Committee of the Regions "Ready for 55": achieving the EU's 2030 climate target on the way to climate neutrality; https://eur-lex.europa.eu/legal-content/PL/TXT/?uri=CELEX%3A52021DC0550 (Accessed: 10.07.2024).
2. Communication from the Commission to the European Parliament, the European Council, the Council, the European Economic and Social Committee and the Committee of the Regions. REPowerEU Plan; https://eur-lex.europa.eu/legal-content/PL/TXT/?uri=CELEX%3A52022DC0230 (Accessed:: 08.06.2024).
3. SolarPower Europe (2023): EU Market Outlook for Solar Power 2023–2027; https://www.solarpowereurope.org/insights/outlooks/eu-market-outlook-for-solar-power-2023-2027/detail (Accessed: 08.06.2024).
4. Raport. Energia elektryczna wytworzona z odnawialnych źródeł energii w mikroinstalacjach (w tym przez prosumentów) i wprowadzana do sieci dystrybucyjnej w 2023r., Urząd Regulacji Energetyki, Warszawa, marzec 2024; https://bip.ure.gov.pl/bip/o-urzedzie/zadania-prezesa-ure/raport-oze-art-6a-ustaw/3793,Raport-dotyczacy-energii-elektrycznej-wytworzonej-z-OZE-w-mikroinstalacji-i-wpro.html (Accessed: 08.06.2024).
5. Muller M.O., Stampfli A., Dold U., Hammer T. Energy autarky: A conceptual framework for sustainable regional development. Energy Policy 2011; 39(10): 5800–5810. https://doi.org/10.1016/j.enpol.2011.04.019
6. Kaldellis J. Optimum technoeconomic energy autonomous photovoltaic solution for remote consumers throughout Greece. Energy Conversion and Management 2004; 45(17): 2745–2760. https://doi.org/10.1016/j.enconman.2003.12.007

7. Kaldellis J.K., Kavadias K.A., Koronakis P.S. Comparing wind and photovoltaic standalone power systems used for the electrification of remote consumers. Renewable and Sustainable Energy Reviews 2007; 11(1): 57–77. https://doi.org/10.1016/j.rser.2004.12.001
8. Kaldellis J.K., Zafirakis D., Kondili E. Energy payback period analysis of stand-alone photovoltaic systems. Renewable Energy 2010; 35(7): 1444–1454. https://doi.org/10.1016/j.renene.2009.12.016
9. Petrakopoulou F., Robinson A., Loizidou M. Simulation and evaluation of a hybrid concentrating-solar and wind power plant for energy autonomy on islands. Renewable Energy 2016; 96(PA): 863–871. https://doi.org/10.1016/j.renene.2016.05.030
10. Petrakopoulou F. On the economics of stand-alone renewable hybrid power plants in remote regions. Energy Conversion and Management 2016; 118: 63–74. https://doi.org/10.1016/j.enconman.2016.03.070
11. Diaf S., Notton G., Belhamel M., Haddadi M., Louche A. Design and technoeconomical optimization for hybrid PV/wind system under various meteorological conditions. Applied Energy 2008; 85(10): 968–987. https://doi.org/10.1016/j.apenergy.2008.02.012
12. Juntunen J. K., Martiskainen M. Improving understanding of energy autonomy: A systematic review. Renewable and Sustainable Energy Reviews 2021; 141: 110797. https://doi.org/10.1016/j.rser.2021.110797
13. Ukoba K., Fadare O., Jen Tien-Chien. Powering Africa using an off-grid, stand-alone, solar photovoltaic model. Journal of Physics: Conference Series 2019; 1378: 022031. https://doi.org/10.1088/1742-6596/1378/2/022031
14. Kaldellis J. Parametrical investigation of the wind – hydro electricity production solution for Aegean Archipelago. Energy Conversion and Management 2002; 43(16): 2097–2113. https://doi.org/10.1016/S0196-8904(01)00168-6
15. Katsaprakakis D., Voumvoulakis M. A hybrid power plant towards 100% energy autonomy for the island of Sifnos, Greece. Perspectives created from energy cooperatives. Energy 2018; 161: 680–698. https://doi.org/10.1016/j.energy.2018.07.198
16. Brosig C., Waffenschmidt E. Energy autarky of households by sufficiency measures. Energy Procedia 2016; 99: 194–203. https://doi.org/10.1016/j.egypro.2016.10.110
17. Russo G., Anifantis A., Verdiani G., Scarascia G. Environmental analysis of geothermal heat pump and LPG greenhouse heating systems. Biosystems Engineering 2014; 127(7): 11–23. https://doi.org/10.1016/j.biosystemseng.2014.08.002
18. Sonneveld P.J., GLAM Swinkels, Campen J., van Tuijl B.A.J., Janssen H.J.J., Bot G.P.A. Performance results of a solar greenhouse combining electrical and thermal energy production. Biosystems Engineering 2010; 106(1): 48–57. https://doi.org/10.1016/j.biosystemseng.2010.02.003
19. Al-Shamiry F., Ahmad D., Sharif R., Aris I., Janius R., Kamaruddin R. Design and development of photovoltaic power system for tropical greenhouse cooling. American Journal of Applied Sciences 2007; 4(6): 386–389. https://doi.org/10.1016/j.solener.2020.01.057
20. Maerefat M., Haghighi A.P. Passive cooling of buildings by using integrated earth to air heat exchanger and solar chimney. Renewable Energy 2010; 35(10): 2316–2324. https://doi.org/10.1016/j.renene.2010.03.003
21. Mongkon S., Thepa S., Namprakai P., Pratinthong N. Cooling performance assessment of horizontal earth tube system and effect on planting in tropical greenhouse. Energy Conversion and Management 2014; 78: 225–236. https://doi.org/10.1016/j.enconman.2013.10.076
22. Hassanien R., Hassanien E., Li M., Dong Lin W. Advanced applications of solar energy in agricultural greenhouses. Renewable and Sustainable Energy Reviews 2016; 54(C): 989–1001. https://doi.org/10.1016/j.rser.2015.10.095
23. Pande P.C., Singh A.K., Ansari S., Vyas S.K., Dave B.K. Design development and testing of a solar PV pump based drip system for orchards. Renewable Energy 2003; 28(3): 385–396. https://doi.org/10.1016/S0960-1481(02)00037-X
24. Boutelhig A., Bakelli Y., Hadj Mahammed I., Hadj Arab A. Performances study of different PV powered DC pump configurations for an optimum energy rating at different heads under the outdoor conditions of a desert area. Energy 2012; 39(1): 33–39. https://doi.org/10.1016/j.energy.2011.10.016
25. Al-Ali A.R., Rehman S., Al-Agili S., Al-Omari M.H., Al-Fayezi M. Usage of photovoltaics in an automated irrigation system. Renewable Energy 2001; 23(1): 17–26. https://doi.org/10.1016/S0960-1481(00)00110-5
26. Haddad S., Benghanem M., Mellit A., Daffallah K.O. ANNs-based modeling and prediction of hourly flow rate of a photovoltaic water pumping system: experimental validation. Renewable Sustainable Energy Reviews 2015; 43: 635–643. https://doi.org/10.1016/j.rser.2014.11.083
27. Ebaid M.S.Y., Qandil H., Hammad M. A unified approach for designing a photovoltaic solar system for the underground water pumping well-34 at Disi aquifer. Energy Conversion and Management 2013; 75: 780–795. https://doi.org/10.1016/j.enconman.2013.07.083
28. Słomczyńska K., Mirek P., Panowski M. Analysis of

the potential for reducing the energy consumption of a vegetable sprouts production using flownex simulation software. Advances in Science and Technology Research Journal 2023; 17(5): 163–173. https://doi.org/10.12913/22998624/170944

29. Słomczyńska K, Mirek P., Panowski M., Saja-Garbarz D., Janeczko A., Skoczowski A. Assessing the feasibility of recovering heat from Mung Bean sprout production for food consumption, Thermochimica Acta, 2024; 731: 179654, https://doi.org/10.1016/j.tca.2023.179654
30. Mirek P., Panowski M., Słomczyńska K., Stanek M., Bąkowski T. Resources and potential for utilization of low-exergy heat from mung bean sprouts cultivation – case study, Archives of thermodynamics, 2023; 44(4): 507–534, https://doi.org/10.24425/ather.2023.149727
31. Słomczyńska K. Wykorzystanie ciepła odpadowego o niskiej egzergii z procesu produkcji kiełków warzywnych, PhD Thesis at Czestochowa University of Technology, Czestochowa, 2024, https://bip.pcz.pl/plik,2264,rozprawa-doktorska.pdf
32. https://www.gov.pl/web/archiwum-inwestycje-rozwoj/dane-do-obliczen-energetycznych-budynkow (Accessed: 30.06.2024)
33. https://re.jrc.ec.europa.eu/pvg_tools/en/#api_5.2 (Accessed: 30.06.2024)